

Article

Tribological Properties of $\text{ZnS}(\text{NH}_2\text{CH}_2\text{CH}_2\text{NH}_2)_{0.5}$ and ZnS as Additives in Lithium Grease

Aoxiang Lu, Wenxing Niu, Yingjing Dai, Hong Xu * and Jinxiang Dong * 

Research Institute of Special Chemicals, College of Chemistry and Chemical Engineering, Taiyuan University of Technology, Taiyuan 030024, China; luaoxiang123@163.com (A.L.); niuwenxing15@163.com (W.N.); daiyingjing930329@163.com (Y.D.)

* Correspondence: xuhongwork@126.com (H.X.); dongjinxiang@tyut.edu.cn (J.D.); Tel.: +86-0351-6010-5508 (H.X. & J.D.)

Received: 10 December 2018; Accepted: 12 March 2019; Published: 20 March 2019



Abstract: The layered compound $\text{ZnS}(\text{NH}_2\text{CH}_2\text{CH}_2\text{NH}_2)_{0.5}$ was evaluated as an additive in grease with different concentrations by using a four-ball tribometer. Results show that $\text{ZnS}(\text{NH}_2\text{CH}_2\text{CH}_2\text{NH}_2)_{0.5}$ grease has good load bearing ability and excellent anti-wear properties. $\text{ZnS}(\text{NH}_2\text{CH}_2\text{CH}_2\text{NH}_2)_{0.5}$ revealed better wear resistance than that of ZnS under all test conditions. The reason for this may be that the two-dimensional structure of $\text{ZnS}(\text{NH}_2\text{CH}_2\text{CH}_2\text{NH}_2)_{0.5}$, with larger interspaces, facilitates an easier sliding process, improving the anti-wear performance. The mechanism was estimated through analysis of the worn surface with SEM, EDS, 3D, and XPS. XPS analysis results show that the tribofilm was mainly composed of FeS, ZnS, ZnO, Fe_xO_y , $\text{Fe}_u(\text{SO}_4)_v$, and ZnSO_4 . Owing to the simple synthetic method and superior tribological properties as a grease-based additive, $\text{ZnS}(\text{NH}_2\text{CH}_2\text{CH}_2\text{NH}_2)_{0.5}$ holds great potential for use in demanding industrial applications in the future.

Keywords: $\text{ZnS}(\text{NH}_2\text{CH}_2\text{CH}_2\text{NH}_2)_{0.5}$; lubricant additive; lithium grease; tribological behavior

1. Introduction

When moving, mechanical parts slide past one another, thus potential wear of the moving surfaces may exist. Unwanted wear may lead to huge losses in terms of materials and energy [1]. The use of solid materials as lubricant additives is very important to reduce friction and wear between the sliding surfaces. To reduce wear, several metal sulfides have been experimentally evaluated through comparative analysis of their tribological behaviors, such as MoS_2 [2–4], WS_2 [5,6], FeS [7], CuS [8], and ZnS [9–18]. Among these metal sulfides, ZnS has been investigated under a wide range of operating conditions in the field of tribology. Liu's group investigated the addition of dialkyldithiophosphate-coated ZnS nanoparticles in liquid paraffin, finding that they effectively reduced wear and showed better load-carrying capacity than that of liquid paraffin [9,10]. The frictional properties of octadecylamine modified ZnS nanorods and nanowires dispersed in dodecane were studied under humidity condition; the coefficient of friction was sensitive to trace amounts of water [11]. Wang et al. reported that polyethylene glycol monomethyl ether dithio phosphate modified ZnS, as an additive in PEG-400, had good anti-wear and friction reduction properties [12]. Zhao reported the tribological performance of the hybrid composite ZnS/short fibers/Polyimide under poly-alpha-olefin (PAO) oil lubrication; fibers imparted abrasion resistance to the composite, and ZnS particles generated a tribochemical film during the sliding [13]. Other researchers noted that the filling of ZnS nanoparticles in the polymer can improve the carrying capacity of the polymer and reduce the friction coefficient, so as to improve the mechanical wear resistance and prolong the service life [14–17]. Kang found that a composite Zn/ZnS coating had excellent friction-reduction and anti-wear properties under dry conditions [18].

Despite the progress made in research, however, most research has focused on oil conditions, and no detailed tribological studies have been devoted to the use of ZnS and its derivatives as additives in grease. Here, we present the friction and wear performance of the organic–inorganic hybrid $\text{ZnS}(\text{NH}_2\text{CH}_2\text{CH}_2\text{NH}_2)_{0.5}$ and hexagonal wurtzite ZnS as grease-based lubricant additives. In the layered structure of $\text{ZnS}(\text{NH}_2\text{CH}_2\text{CH}_2\text{NH}_2)_{0.5}$, the layer is similar to wurtzite ZnS; the layers themselves are connected through the bonding of the nitrogen atoms present in ethylenediamine [19]. Compared with the wurtzite ZnS structure, the layered crystalline structure of $\text{ZnS}(\text{NH}_2\text{CH}_2\text{CH}_2\text{NH}_2)_{0.5}$ may have different tribological performance.

In this paper, $\text{ZnS}(\text{NH}_2\text{CH}_2\text{CH}_2\text{NH}_2)_{0.5}$ was synthesized by the solvothermal method in the presence of ethylenediamine [20]. The pure wurtzite phase of ZnS was gained by annealing $\text{ZnS}(\text{NH}_2\text{CH}_2\text{CH}_2\text{NH}_2)_{0.5}$ at 350 °C for 60 min. The obtained ZnS had the same size and shape as $\text{ZnS}(\text{NH}_2\text{CH}_2\text{CH}_2\text{NH}_2)_{0.5}$ by this method. The tribological properties of ZnS and $\text{ZnS}(\text{NH}_2\text{CH}_2\text{CH}_2\text{NH}_2)_{0.5}$ as additives in lithium grease were investigated by using a four-ball tester under the same test conditions. The three-dimensional (3D) optical profiler, X-ray photoelectron spectroscopy (XPS), was used to characterize the impact of ZnS and $\text{ZnS}(\text{NH}_2\text{CH}_2\text{CH}_2\text{NH}_2)_{0.5}$ on tribological performance.

2. Experimental Section

2.1. Chemicals

Zinc chloride (ZnCl_2 , ≥ 98.0 wt %), ethylenediamine ($\text{C}_2\text{H}_8\text{N}_2$, ≥ 98.0 wt %), sulfur (S, 99.5 wt %), petroleum ether (Sinopharm Group Chemical Reagent Co., Ltd.), 12-hydroxy stearic acid (>75 wt %), and stearic acid (>98 wt %) (TCI (Shanghai) Development Co., Ltd., Shanghai, China) were used. A commercial poly-alpha-olefin PAO8 (viscosity of 46.48 mm^2/s at 40 °C, viscosity index of 146, Exxon Mobil Corp, Clinton, NJ, USA) was used. All chemicals and base oils were obtained from commercial sources and were used as received. Distilled water (H_2O) was prepared in our laboratory.

2.2. Synthesis of $\text{ZnS}(\text{NH}_2\text{CH}_2\text{CH}_2\text{NH}_2)_{0.5}$, ZnS, and the Grease Samples

$\text{ZnS}(\text{NH}_2\text{CH}_2\text{CH}_2\text{NH}_2)_{0.5}$ was prepared by the conventional solvent thermal method [20]. In a typical synthesis process, 1.228 g zinc chloride was added to 20 mL ethylenediamine, and the mixture was stirred for about 5 min. Once the mixture was homogeneous, 0.384 g sulfur was added to the mixture. With continuous stirring for 10 min, the mixture was transferred to a 30 mL Teflon-lined stainless steel autoclave, sealed, and maintained at 180 °C for 3 days in an electric oven. The crystalline products were washed with distilled water and dried at room temperature. ZnS was obtained by annealing $\text{ZnS}(\text{NH}_2\text{CH}_2\text{CH}_2\text{NH}_2)_{0.5}$ at 350 °C for 60 min.

The lithium-based grease was prepared according to the previous literature [21]. Different concentrations (1.0–7.0 wt %) of $\text{ZnS}(\text{NH}_2\text{CH}_2\text{CH}_2\text{NH}_2)_{0.5}$ and ZnS materials were added to the lithium-based grease and then stirred and rolled three times in a triple-roller mill.

2.3. Material Characterization and Tribological Tests

The crystallinity and phase purity of $\text{ZnS}(\text{NH}_2\text{CH}_2\text{CH}_2\text{NH}_2)_{0.5}$ and ZnS samples were analyzed by powder X-ray diffraction (XRD) on a Rigaku MiniflexII diffractometer with Cu $\text{K}\alpha$ radiation ($\lambda = 1.5418 \text{ \AA}$) at 30 kV and 15 mA. A Hitachi, SU8010 Scanning Electron Microscope (SEM) was used to record the powder samples.

The tribological test was performed using a Four Ball Tester (Xiamen Tenkey Co., Ltd. Xiamen, China). The test balls ($\text{Ø} 12.7$ mm, HRC 60 ± 1) were made of GCr15. The maximum nonseizure load (P_B) and weld load (P_D) tests were measured as the Chinese national standard GB/T3142-90, which is similar to ASTM D2783-03. General tribological tests were conducted under different applied loads (294 N, 392 N, 490 N, and 588 N) with a rotating speed of 300 rpm or 1450 rpm for a time duration of

30 min at 75 °C. A microscope was used to determine the wear scar diameter of the lower three balls. The friction coefficients were measured after each test.

The worn surfaces of the lower steel balls were investigated by using a three-dimensional (3D) non-contact optical profiling system (Zygo, Zegage), and scanning electron microscopy (SEM) at 5 KV (Hitachi, TM-3000, Tokyo, Japan). X-ray photoelectron spectroscopy (XPS) was used to observe the chemical states of chemicals of the lower steel balls, which was accomplished using an AXIS Ultra DLD X-ray photoelectron spectrometer with Al K α line excitation source.

3. Results and Discussion

3.1. Characterizations of $\text{ZnS}(\text{NH}_2\text{CH}_2\text{CH}_2\text{NH}_2)_{0.5}$ and ZnS

Figure S1 shows the XRD patterns of the synthesized $\text{ZnS}(\text{NH}_2\text{CH}_2\text{CH}_2\text{NH}_2)_{0.5}$ under different reaction conditions. The XRD pattern of the as-synthesized $\text{ZnS}(\text{NH}_2\text{CH}_2\text{CH}_2\text{NH}_2)_{0.5}$ is shown in Figure 1a; the diffraction peaks matched well with patterns found in the literature [20]. The pure wurtzite phase of ZnS was produced by annealing $\text{ZnS}(\text{NH}_2\text{CH}_2\text{CH}_2\text{NH}_2)_{0.5}$. The XRD patterns of $\text{ZnS}(\text{NH}_2\text{CH}_2\text{CH}_2\text{NH}_2)_{0.5}$, annealed under different temperatures for 60 min, are shown in Figure 1a. The pure wurtzite phase of ZnS was produced as a result of decomposition of ethylenediamine molecules. The product purity of ZnS significantly depended on the calcination temperature and time (Figure S2). As the temperature increased, the intensity of XRD diffraction peaks of ZnS gradually strengthened. When the temperature reached 350 °C, only peaks of ZnS were detected, indicating that $\text{ZnS}(\text{NH}_2\text{CH}_2\text{CH}_2\text{NH}_2)_{0.5}$ was completely transformed into ZnS, as shown in Figure 1b. The peak positions were in agreement with the standard wurtzite structure of ZnS (JCPDS No. 36-1450). In Figure 2, it can be seen that $\text{ZnS}(\text{NH}_2\text{CH}_2\text{CH}_2\text{NH}_2)_{0.5}$ and ZnS had the same sheet-like shape and size. The obtained particle size was about 3.0–5.0 μm .

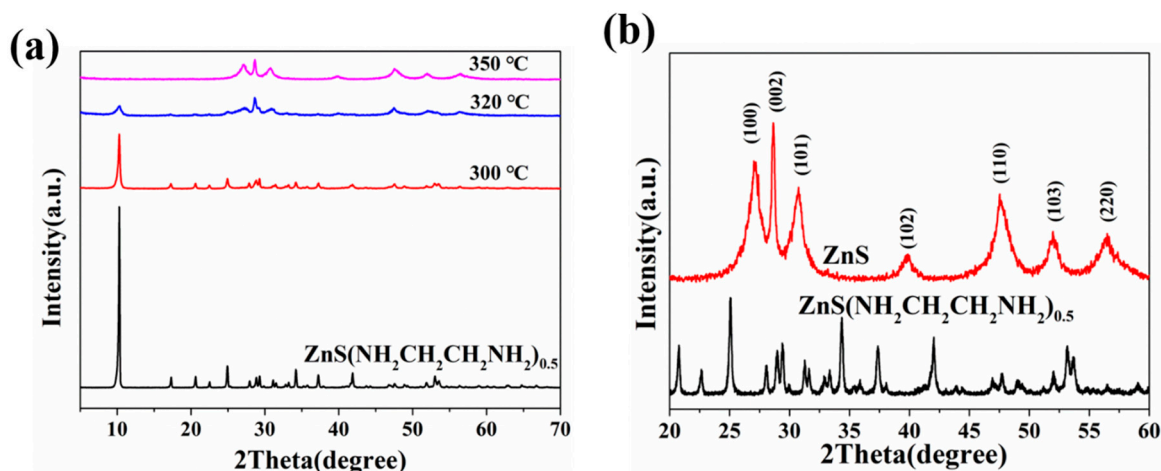


Figure 1. XRD patterns: (a) $\text{ZnS}(\text{NH}_2\text{CH}_2\text{CH}_2\text{NH}_2)_{0.5}$ and its derivatives annealed for 60 min at different temperatures; and (b) magnification pattern of $\text{ZnS}(\text{NH}_2\text{CH}_2\text{CH}_2\text{NH}_2)_{0.5}$ and ZnS obtained by annealing $\text{ZnS}(\text{NH}_2\text{CH}_2\text{CH}_2\text{NH}_2)_{0.5}$ at 350 °C.

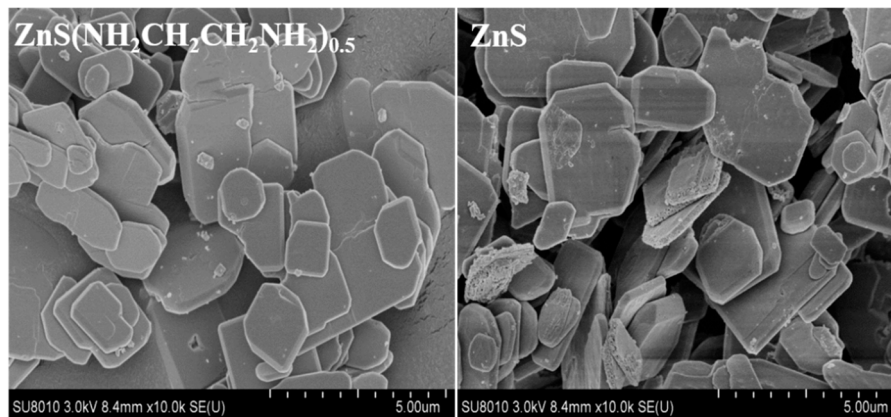


Figure 2. The SEM images of: $\text{ZnS}(\text{NH}_2\text{CH}_2\text{CH}_2\text{NH}_2)_{0.5}$ (left); and ZnS (right).

3.2. Tribological Properties of $\text{ZnS}(\text{NH}_2\text{CH}_2\text{CH}_2\text{NH}_2)_{0.5}$ and ZnS

Figure 3 gives the tribological behavior as a function of the additive concentration of $\text{ZnS}(\text{NH}_2\text{CH}_2\text{CH}_2\text{NH}_2)_{0.5}$ and ZnS under the load of 294 N. Figure 3a,b presents the maximum non-seizure load (P_B) and the sintered load (P_D) values of lithium grease containing different concentrations of $\text{ZnS}(\text{NH}_2\text{CH}_2\text{CH}_2\text{NH}_2)_{0.5}$ and ZnS . The results show that the values increased gradually with the increase of the additive concentration. Both $\text{ZnS}(\text{NH}_2\text{CH}_2\text{CH}_2\text{NH}_2)_{0.5}$ and ZnS were capable of improving the P_B and P_D values of the base grease, and the values of ZnS were higher than those of $\text{ZnS}(\text{NH}_2\text{CH}_2\text{CH}_2\text{NH}_2)_{0.5}$ at each concentration. When the additive concentration was 5.0 wt %, the P_B values for $\text{ZnS}(\text{NH}_2\text{CH}_2\text{CH}_2\text{NH}_2)_{0.5}$ and ZnS were 882 N and 1372 N, respectively. The P_D values for $\text{ZnS}(\text{NH}_2\text{CH}_2\text{CH}_2\text{NH}_2)_{0.5}$ and ZnS were 1568 N and 2450 N, respectively. Obviously, ZnS performed significantly better than $\text{ZnS}(\text{NH}_2\text{CH}_2\text{CH}_2\text{NH}_2)_{0.5}$ in enhancing the load-carrying capacity and extreme pressure properties of base grease. In Figure 3c, it can be noted that the variation tendency of the wear scar diameters (WSD) lubricated by the lithium grease containing $\text{ZnS}(\text{NH}_2\text{CH}_2\text{CH}_2\text{NH}_2)_{0.5}$ and ZnS was different. The WSD values for $\text{ZnS}(\text{NH}_2\text{CH}_2\text{CH}_2\text{NH}_2)_{0.5}$ grease were lower than those of pure lithium grease at all concentrations. The higher was the $\text{ZnS}(\text{NH}_2\text{CH}_2\text{CH}_2\text{NH}_2)_{0.5}$ concentration in lithium grease, the lower was the corresponding WSD values, whereas the WSD values for ZnS grease increased with the increase of ZnS concentration. These results show that $\text{ZnS}(\text{NH}_2\text{CH}_2\text{CH}_2\text{NH}_2)_{0.5}$ had better anti-wear properties than did ZnS under the same concentration. Figure 3d shows the friction coefficient as a function of the additive concentration. The friction coefficient of the lithium grease containing $\text{ZnS}(\text{NH}_2\text{CH}_2\text{CH}_2\text{NH}_2)_{0.5}$ and ZnS had little variation with the increase of the concentration in the range of 1.0–7.0 wt %. The friction coefficient of $\text{ZnS}(\text{NH}_2\text{CH}_2\text{CH}_2\text{NH}_2)_{0.5}$ grease was more stable than that of $\text{ZnS}(\text{NH}_2\text{CH}_2\text{CH}_2\text{NH}_2)_{0.5}$ grease at the test concentrations.

The above results show that the lithium grease containing $\text{ZnS}(\text{NH}_2\text{CH}_2\text{CH}_2\text{NH}_2)_{0.5}$ and ZnS exhibited different tribological features. Solid lubricants, used as additives, provide enhanced lubrication for many different types of applications, such as low or high sliding speeds under high loads [22]. To better understand the anti-wear (AW) and the extreme pressure (EP) property differences between the two materials, this study was divided into two stages. The first stage was conducted under different applied loads (294 N, 392 N, 490 N, and 588 N) at 75 °C for a time duration of 30 min; the rotating speed was conducted at a low speed (300 r/min) and a high speed (1450 r/min), respectively. The aim of this stage was to evaluate effectiveness of $\text{ZnS}(\text{NH}_2\text{CH}_2\text{CH}_2\text{NH}_2)_{0.5}$ and ZnS on the AW/EP characteristics under different applied loads at a low speed and a high speed, respectively. In the second stage, the time duration was extended from 30 to 120 min, and the choice of the applied load was determined by ensuring that both $\text{ZnS}(\text{NH}_2\text{CH}_2\text{CH}_2\text{NH}_2)_{0.5}$ and ZnS grease could run under the highest given load. The aim of this stage was to evaluate the anti-wear property of $\text{ZnS}(\text{NH}_2\text{CH}_2\text{CH}_2\text{NH}_2)_{0.5}$ and ZnS under high applied loads over an extended period. Based on

the obtained results shown in Figure 3, the concentration of $\text{ZnS}(\text{NH}_2\text{CH}_2\text{CH}_2\text{NH}_2)_{0.5}$ and ZnS as additives in lithium grease was suggested to be 5.0 wt %.

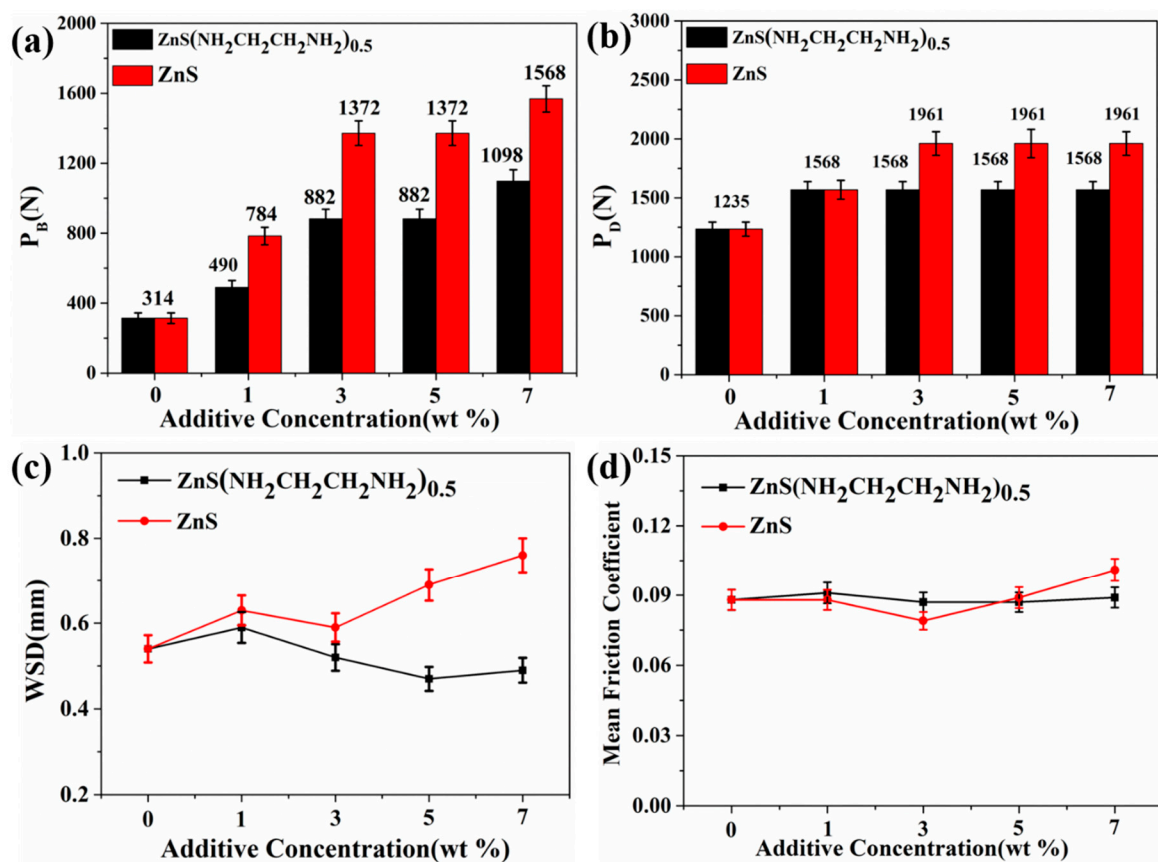


Figure 3. (a) The maximum non-seizure; (b) weld point load; (c) wear scar diameter (WSD); and (d) mean friction coefficient as a function of the concentration of $\text{ZnS}(\text{NH}_2\text{CH}_2\text{CH}_2\text{NH}_2)_{0.5}$ and ZnS (four-ball tester, applied load 294 N, rotary speed 1450 rpm, duration 30 min).

The tribological properties of $\text{ZnS}(\text{NH}_2\text{CH}_2\text{CH}_2\text{NH}_2)_{0.5}$ and ZnS grease were evaluated at the rotating speed of 300 rpm, and different loads (294, 392, and 490 N) were applied to determine the maximum applied load under which the grease could still function. As shown in Figure 4a, the maximum applied load for $\text{ZnS}(\text{NH}_2\text{CH}_2\text{CH}_2\text{NH}_2)_{0.5}$ grease was 490 N, which was 1.25 times that of the ZnS grease. The WSD values for $\text{ZnS}(\text{NH}_2\text{CH}_2\text{CH}_2\text{NH}_2)_{0.5}$ were 0.38 mm, 0.42 mm, and 0.47 mm, respectively, and the values corresponding to ZnS were 0.48 mm and 0.51 mm, respectively. The WSD values of $\text{ZnS}(\text{NH}_2\text{CH}_2\text{CH}_2\text{NH}_2)_{0.5}$ were obviously lower than those of ZnS under the same applied load. The 3D images in Figure 4b show that the wear scars lubricated by $\text{ZnS}(\text{NH}_2\text{CH}_2\text{CH}_2\text{NH}_2)_{0.5}$ were small and shallow, whereas the scars lubricated by ZnS were large and deep, displaying more grooves. In Figure 4c, it can be seen that the dynamic friction coefficient of $\text{ZnS}(\text{NH}_2\text{CH}_2\text{CH}_2\text{NH}_2)_{0.5}$ displayed a declining trend as friction time went on, fluctuating between 0.08 and 0.11, while the dynamic friction coefficient of ZnS gradually increased as time went on, fluctuating between 0.08 and 0.12.

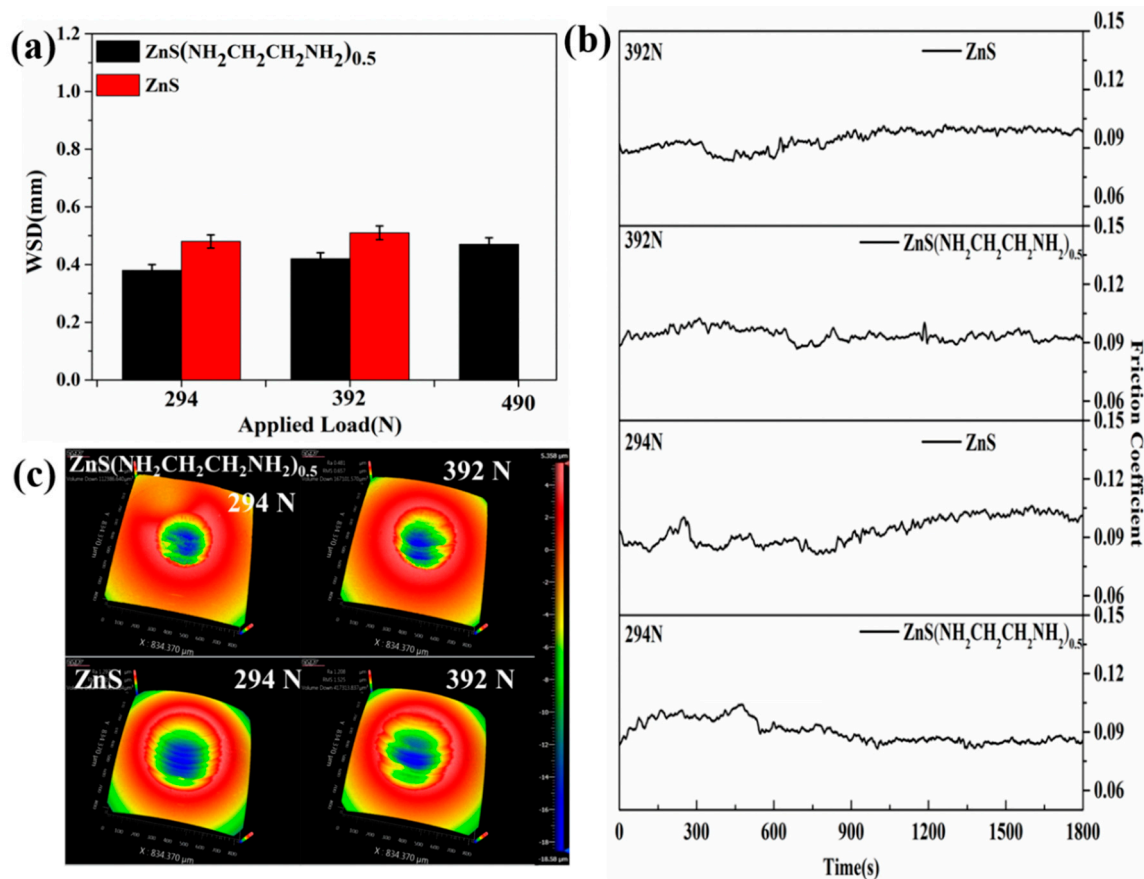


Figure 4. (a) wear scar diameter; (b) 3D microscopic images; and (c) dynamic friction coefficient curves for the lithium grease containing 5.0 wt % ZnS(NH₂CH₂CH₂NH₂)_{0.5} and 5.0 wt % ZnS under different applied loads (four-ball tester, rotary speed 300 rpm, duration 30 min).

When the rotating speed increased to 1450 rpm, the maximum applied load for ZnS(NH₂CH₂CH₂NH₂)_{0.5} grease was 490 N, and, for ZnS grease, it was 588 N. ZnS could support a higher load than ZnS(NH₂CH₂CH₂NH₂)_{0.5} at the high rotating speed (Figure 5a). The variation tendency of WSD was similar to the rotating speed at 300 rpm; the WSD values of ZnS(NH₂CH₂CH₂NH₂)_{0.5} were still lower than those of ZnS under each applied load. As shown in Figure 5b, the corresponding 3D images of ZnS grease showed more scratch marks than those of ZnS(NH₂CH₂CH₂NH₂)_{0.5} grease on the worn surface. The dynamic friction coefficient curve of ZnS(NH₂CH₂CH₂NH₂)_{0.5} grease was relatively steady throughout the test.

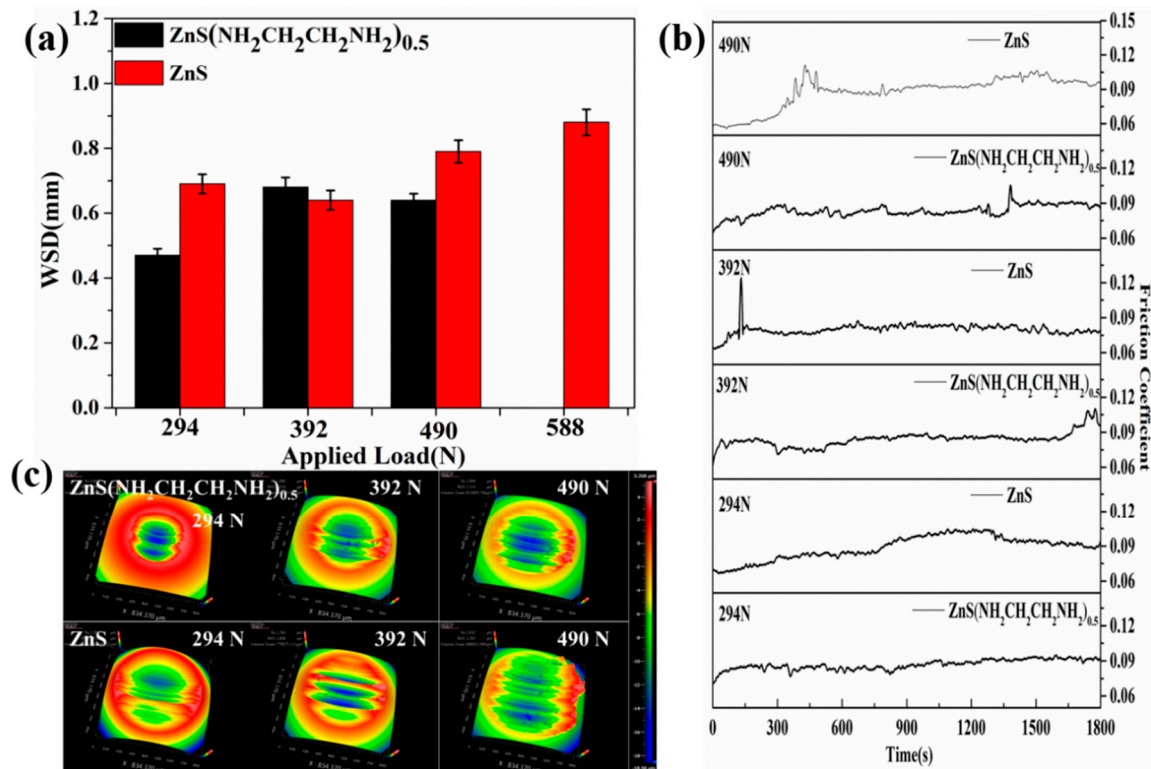


Figure 5. (a) wear scar diameter; (b) 3D microscopic images; and (c) dynamic friction coefficient curves for the lithium grease containing 5.0 wt % ZnS(NH₂CH₂CH₂NH₂)_{0.5} and 5.0 wt % ZnS under different applied loads (four-ball tester, rotary speed 1450 rpm, duration 30 min).

The maximum applied load under which the two grease samples could run at 300 rpm for 30 min was 392 N. The evaluation of long-time tribological properties for 5.0 wt % ZnS(NH₂CH₂CH₂NH₂)_{0.5} grease and 5.0 wt % ZnS grease was carried out under 392 N at 300 rpm for 120 min. Through analysis of each surface after testing, the 3D SEM images and the profiles of wear scars of lower balls are shown in Figure 6. With the prolonged time, all values of wear scar diameter and wear depth increased accordingly; the values of WSD and the maximum wear depth for ZnS(NH₂CH₂CH₂NH₂)_{0.5} grease were 0.53 mm and 7.06 μ m, respectively, while, for ZnS grease, the values were 0.78 mm and 8.93 μ m, respectively. The 3D images show that the wear values of ZnS(NH₂CH₂CH₂NH₂)_{0.5} were clearly lower than those of ZnS; the amount of wear for ZnS was higher, and deep scratches could be observed on the wear scar of the ball.

The tribological properties of 5.0 wt % ZnS(NH₂CH₂CH₂NH₂)_{0.5} grease and 5.0 wt % ZnS grease were also determined under 490 N at 1450 rpm for 120 min, as shown in Figure 7. The maximum applied load under which the two grease samples could run through the whole test was 490 N. The variation tendency of wear values was similar to the rotating speed at 300 rpm, and the WSD value and the maximum wear depth of ZnS(NH₂CH₂CH₂NH₂)_{0.5} were still lower than those of ZnS. The values of WSD and the maximum wear depth for ZnS(NH₂CH₂CH₂NH₂)_{0.5} grease were 0.88 mm and 21.50 μ m, respectively, while, for ZnS grease, the values were 1.03 mm and 23.53 μ m, respectively. From SEM and 3D images, it is apparent that wear tracks with ZnS grease were relatively wider and deeper than the ones lubricated by ZnS(NH₂CH₂CH₂NH₂)_{0.5} grease; sharp furrows existed on the wear track, which further confirmed the superiority of the anti-wear properties of ZnS(NH₂CH₂CH₂NH₂)_{0.5}.

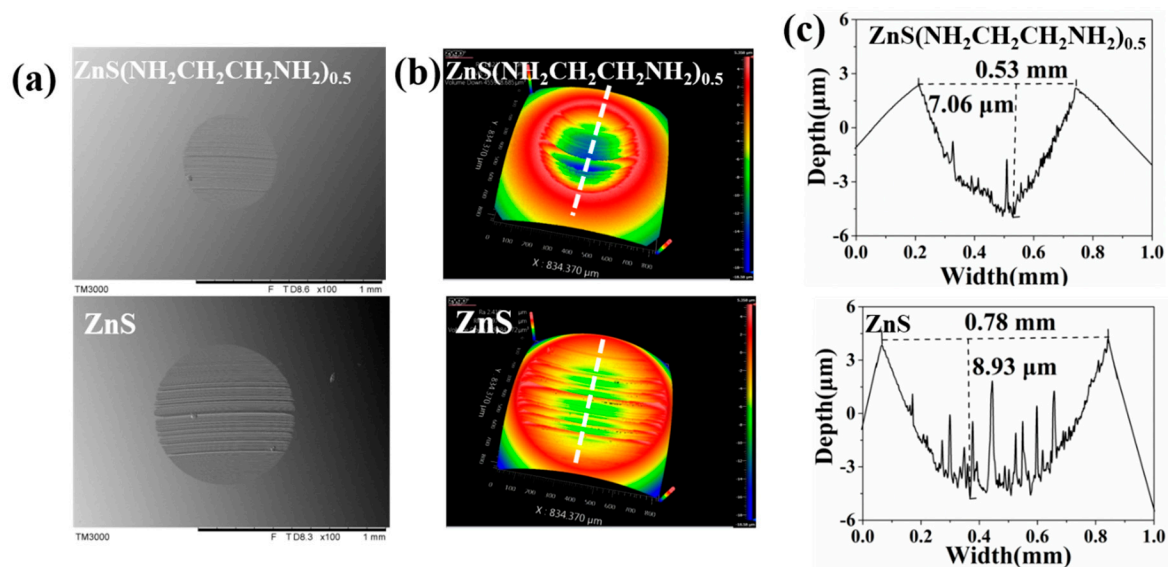


Figure 6. (a) SEM images, (b) 3D microscopic images, and (c) the profiles of wear scars of lower balls for the lithium grease containing 5.0 wt % $\text{ZnS}(\text{NH}_2\text{CH}_2\text{CH}_2\text{NH}_2)_{0.5}$ and 5.0 wt % ZnS (four-all tester, applied load 392 N, rotary speed 300 rpm, duration 120 min).

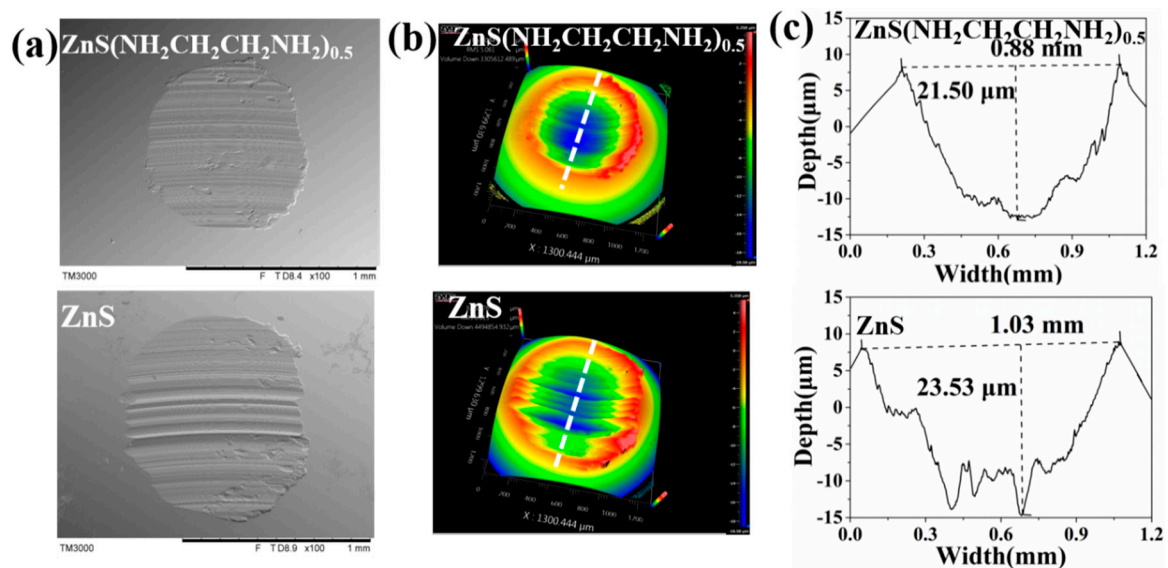


Figure 7. (a) SEM images, (b) 3D microscopic images, and (c) the profiles of wear scars of lower balls for the lithium grease containing 5.0 wt % $\text{ZnS}(\text{NH}_2\text{CH}_2\text{CH}_2\text{NH}_2)_{0.5}$ and 5.0 wt % ZnS (four-ball tester, applied load 490 N, rotary speed 1450 rpm, duration 120 min).

All the above results indicate that the anti-wear properties of $\text{ZnS}(\text{NH}_2\text{CH}_2\text{CH}_2\text{NH}_2)_{0.5}$ were better than those of ZnS under all listed test conditions. $\text{ZnS}(\text{NH}_2\text{CH}_2\text{CH}_2\text{NH}_2)_{0.5}$ had higher load-carrying capacity at the low rotating speed, but ZnS had higher load-carrying capacity at the high rotating speed.

3.3. XPS Analyses of Worn Surface and Tribofilm

Figures 8 and 9 show the S 2p, O 1s, Fe 2p, and Zn 2p3 XPS spectra of the counterpart steel ball surface after being slid against ZnS and $\text{ZnS}(\text{NH}_2\text{CH}_2\text{CH}_2\text{NH}_2)_{0.5}$ grease. As shown in Figure 8, the S 2p peak at 161.4 and 162.6 eV can be assigned as sulfide (FeS and ZnS) [23], and the peak between 166.5 and 171.0 eV can be attributed to sulfate radical (SO_4^{2-}). Since the peak width at half-height between 166.5 and 171.0 eV was larger than 3.5 eV, it can be speculated that there were two kinds of

sulfates ($\text{Fe}_u(\text{SO}_4)_v$ and ZnSO_4) [13,23,24]. For O 1s, the peak at 530.0 eV indicated the existence of metal oxides (ZnO and Fe_xO_y) [24,25], and the peak at 531.7 eV can be assigned as sulfates ($\text{Fe}_u(\text{SO}_4)_v$ and ZnSO_4) [13]. It can be seen that Fe 2p had a weak peak at 707.0 eV, indicating that the surface contained a small amount of Fe. Based on the results of S 2p and O 1s, the surface was covered by FeS, ZnS, ZnO, Fe_xO_y , $\text{Fe}_u(\text{SO}_4)_v$, and ZnSO_4 . Comparing Figures 8 and 9, it can be seen that the S 2p, O 1s, Fe 2p, and Zn 2p3 XPS spectra of ZnS grease were similar to the corresponding peak of $\text{ZnS}(\text{NH}_2\text{CH}_2\text{CH}_2\text{NH}_2)_{0.5}$ grease, showing that there were similar compounds on the steel ball surface after being slid against ZnS and $\text{ZnS}(\text{NH}_2\text{CH}_2\text{CH}_2\text{NH}_2)_{0.5}$ grease. In general, metal oxides, metal sulfides, and metal sulfates were formed on the surface of the steel ball after being slid against ZnS and $\text{ZnS}(\text{NH}_2\text{CH}_2\text{CH}_2\text{NH}_2)_{0.5}$ grease.

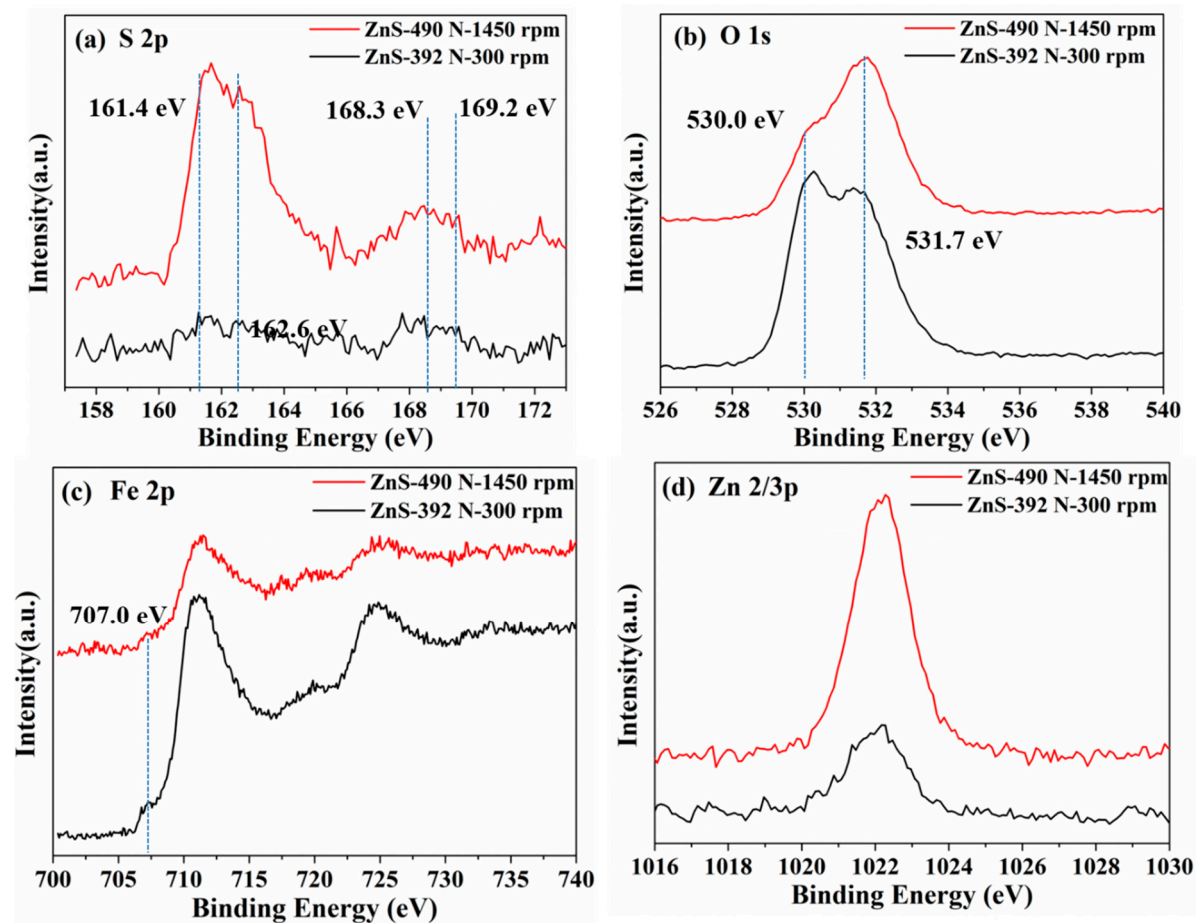


Figure 8. XPS spectra of counterpart steel ball surface after being slid against ZnS grease (four-ball tester, duration 120 min).

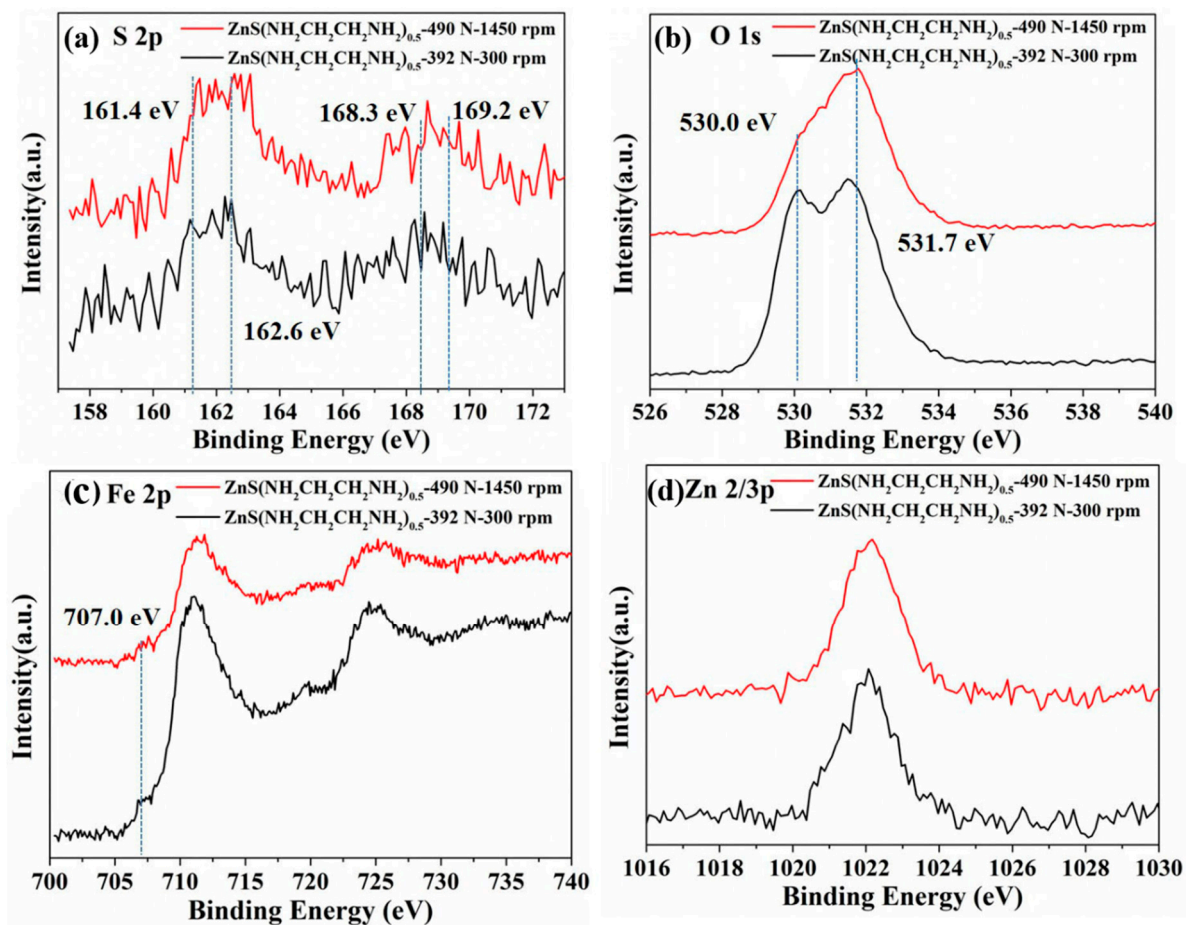


Figure 9. XPS spectra of counterpart steel ball surface after being slid against $\text{ZnS}(\text{NH}_2\text{CH}_2\text{CH}_2\text{NH}_2)_{0.5}$ grease (four-ball tester, duration 120 min).

Tables 1 and 2 show the content of elements detected on the worn surface of the ball counterpart after being slid against ZnS and $\text{ZnS}(\text{NH}_2\text{CH}_2\text{CH}_2\text{NH}_2)_{0.5}$ grease by XPS. As shown in Tables 1 and 2, S and Zn contents on the surface and in the bulk of the ball increased with increased rotation speed (300 vs. 1450 rpm) after being slid against ZnS and $\text{ZnS}(\text{NH}_2\text{CH}_2\text{CH}_2\text{NH}_2)_{0.5}$ grease; on the contrary, Fe content decreased. The result shows that high rotating speed exacerbated the adhesion and chemical reaction. Comparing the contents after being slid against ZnS and $\text{ZnS}(\text{NH}_2\text{CH}_2\text{CH}_2\text{NH}_2)_{0.5}$ grease, the contents of S and Zn on the surface were similar under 300 rpm, but the contents of S and Zn in the bulk after being slid against $\text{ZnS}(\text{NH}_2\text{CH}_2\text{CH}_2\text{NH}_2)_{0.5}$ grease were slightly smaller than those after being slid against ZnS grease. Under 1450 rpm, the contents of S and Zn on the surface and in the bulk after being slid against $\text{ZnS}(\text{NH}_2\text{CH}_2\text{CH}_2\text{NH}_2)_{0.5}$ grease were clearly smaller than those after being slid against ZnS grease. The results indicate that $\text{ZnS}(\text{NH}_2\text{CH}_2\text{CH}_2\text{NH}_2)_{0.5}$ grease restrained the adhesion and chemical reaction on the surface, and the inhibition was more obvious with increased rotation speed. This further proves that the abrasion resistance of the $\text{ZnS}(\text{NH}_2\text{CH}_2\text{CH}_2\text{NH}_2)_{0.5}$ was better than that of ZnS.

In summary, it can be concluded that the chemical reaction occurs between ZnS or $\text{ZnS}(\text{NH}_2\text{CH}_2\text{CH}_2\text{NH}_2)_{0.5}$ and the surface of the friction pair at both low speed and high speed ($\text{ZnS} + \text{Fe} + \text{O}_2 = \text{ZnO} + \text{ZnSO}_4 + \text{Fe}_x\text{O}_y + \text{FeS} + \text{Fe}_u(\text{SO}_4)_v$) [9].

Table 1. Content of elements detected on the worn surface of ball counterpart (Atomic % ¹).

Element	ZnS ^a	ZnS ^b
	XPS	XPS
S	2.07	9.30
O	81.95	72.63
Fe	13.43	9.63
Zn	2.54	8.44

^a 392 N, 300 rpm; ^b 490 N, 1450 rpm; ¹ data normalization.

Table 2. Content of elements detected on the worn surface of ball counterpart (Atomic % ¹).

Element	ZnS(NH ₂ CH ₂ CH ₂ NH ₂) _{0.5} ^a	ZnS(NH ₂ CH ₂ CH ₂ NH ₂) _{0.5} ^b
	XPS	XPS
S	2.36	3.81
O	82.92	82.51
Fe	12.29	9.98
Zn	2.43	3.71

^a 392 N, 300 rpm; ^b 490 N, 1450 rpm; ¹ data normalization.

Based on the tribological test results and surface analysis by SEM and XPS presented above, it can be concluded that the anti-wear properties of ZnS(NH₂CH₂CH₂NH₂)_{0.5} were obviously better than those of ZnS under all the listed test conditions. The difference in anti-wear properties between ZnS(NH₂CH₂CH₂NH₂)_{0.5} and ZnS may be related to their crystal structures. To better understand the tribological performance of ZnS(NH₂CH₂CH₂NH₂)_{0.5} and ZnS as additives in the grease, Figure 10 shows the relevant schematic diagram of the possible tribological mechanism. The hexagonal wurtzite ZnS structure polytypes are formed by the stacking of ABAB forms; the alternating planes can be described as Zn atoms tetrahedrally coordinated by three S atoms [26].

ZnS(NH₂CH₂CH₂NH₂)_{0.5} is an ethylenediamine pillared ZnS layered compound [27]. In the layered structure of ZnS(NH₂CH₂CH₂NH₂)_{0.5}, Zn and S atoms on each layer are closely packed, and the adjacent layers are relatively far apart, resulting from ethylenediamine intercalation; wide interlayer spacing ensures easy shearing or slippage.

When a force is applied perpendicular to the crystallite of ZnS(NH₂CH₂CH₂NH₂)_{0.5}, the wide interlayer spacing between the planes allows for easy shearing of the planes in the direction of the force, resulting in a lamellar mechanism of lubrication [22]. It was observed that the applied loads and the rotating speeds only exerted a slight influence on the anti-wear properties of ZnS(NH₂CH₂CH₂NH₂)_{0.5} (Figures 4 and 5). The worn surface lubricated with ZnS(NH₂CH₂CH₂NH₂)_{0.5} grease was smoother and the furrows became shallower than those of ZnS grease, revealing the better friction-reducing and anti-wear properties under the test conditions. For ZnS, as the force was applied perpendicular to the crystallite, strong interatomic bonding provided high strength and resilience, and the high resilience provided high load-carrying capacity for ZnS, especially at high rotating speed. As shown in Figure 5, the maximum applied load of ZnS grease was 588 N, which was about 17% higher than that of ZnS(NH₂CH₂CH₂NH₂)_{0.5} grease.

The XPS analysis of the corresponding worn steel surface after the long duration test indicated that boundary tribofilms consisted of FeS, ZnS, ZnO, Fe_xO_y, Fe_u(SO₄)_v, and ZnSO₄ tribochemical products. There was no significant difference in the components of ZnS(NH₂CH₂CH₂NH₂)_{0.5} and ZnS. In summary, a lubrication model of ZnS(NH₂CH₂CH₂NH₂)_{0.5} and ZnS additives in the sliding process is proposed. During the sliding process, ZnS(NH₂CH₂CH₂NH₂)_{0.5} and ZnS particles gradually deposited on the rubbing surface; tribochemical reactions took place under the rigorous test conditions.

The tribofilm was composed of tribochemical products and the adsorbed additives. The tribofilm prevented direct steel ball to steel ball contact. It is believed that the crystal structure and the tribochemical reactions of $\text{ZnS}(\text{NH}_2\text{CH}_2\text{CH}_2\text{NH}_2)_{0.5}$ and ZnS are important for maintenance of the lubricating tribofilm when subjected to interfacial rubbing stress.

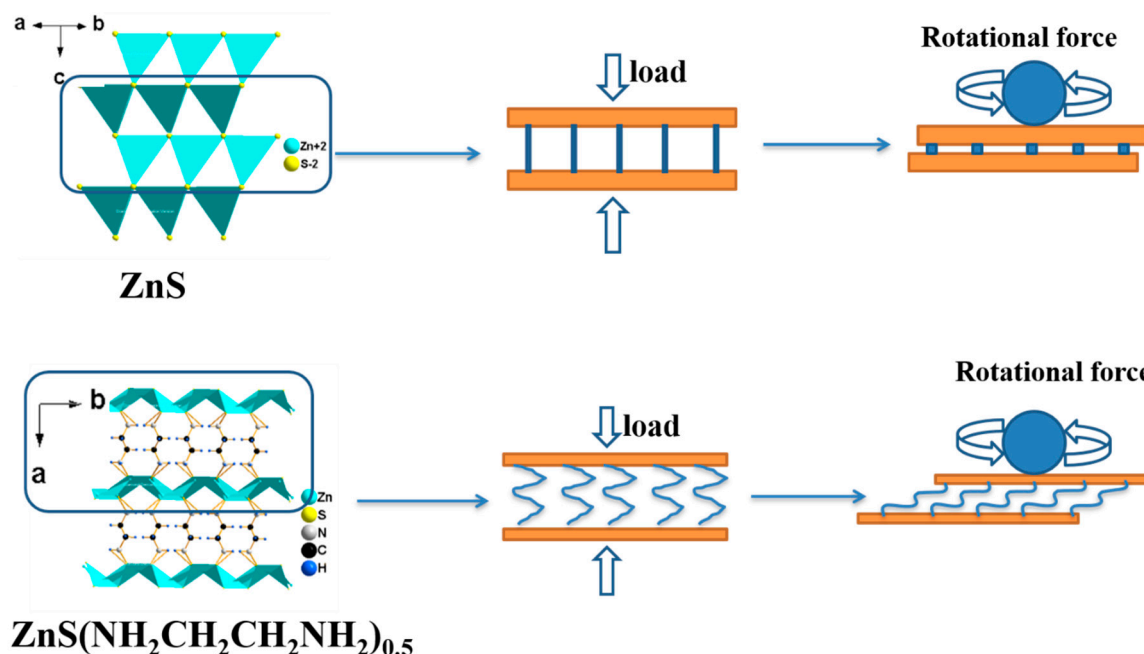


Figure 10. Schematic illustrations of the mechanism for lithium grease with ZnS and $\text{ZnS}(\text{NH}_2\text{CH}_2\text{CH}_2\text{NH}_2)_{0.5}$ as additives.

4. Conclusions

In this paper, $\text{ZnS}(\text{NH}_2\text{CH}_2\text{CH}_2\text{NH}_2)_{0.5}$ was synthesized via the solvent thermal method and wurtzite ZnS was obtained by using a simple thermal annealing technique. $\text{ZnS}(\text{NH}_2\text{CH}_2\text{CH}_2\text{NH}_2)_{0.5}$ and ZnS have the same sheet-like shape and size. The effect of the lithium grease with $\text{ZnS}(\text{NH}_2\text{CH}_2\text{CH}_2\text{NH}_2)_{0.5}$ and ZnS as lubricant additives on the tribological properties was comprehensively studied at different applied loads and sliding speeds. Results show that $\text{ZnS}(\text{NH}_2\text{CH}_2\text{CH}_2\text{NH}_2)_{0.5}$ and ZnS exhibited good performance in terms of load-carrying capacity and extreme pressure properties. $\text{ZnS}(\text{NH}_2\text{CH}_2\text{CH}_2\text{NH}_2)_{0.5}$ showed good and stable anti-wear performance under all test conditions. This was mainly because of the two-dimensional structure of $\text{ZnS}(\text{NH}_2\text{CH}_2\text{CH}_2\text{NH}_2)_{0.5}$, with ethylenediamine intercalation. During the friction process, $\text{ZnS}(\text{NH}_2\text{CH}_2\text{CH}_2\text{NH}_2)_{0.5}$ and ZnS particles were deposited on the rubbing surface. From XPS analysis of the corresponding worn steel surface, it could be seen that the tribofilm was mainly composed of FeS , ZnS , ZnO , Fe_xO_y , $\text{Fe}_u(\text{SO}_4)_v$, and ZnSO_4 .

Supplementary Materials: The following are available online at <http://www.mdpi.com/2075-4442/7/3/26/s1>. Figure S1: XRD patterns of the products obtained under different reaction conditions: (a) the molar ratio of Zn/S = 0.5:1 to 1.5:1 (180 °C, 3 day); and (b) reaction temperatures (Zn/S = 0.75:1, 3 day). Figure S2: XRD patterns of $\text{ZnS}(\text{NH}_2\text{CH}_2\text{CH}_2\text{NH}_2)_{0.5}$ and its derivatives annealed at 350 °C for different time.

Author Contributions: J.D., H.X. and A.L. conceived and designed the experiments; A.L. performed the experiments and analyzed the data; and A.L. and H.X. wrote the paper.

Acknowledgments: This work was supported by the Key Program of National Natural Science Foundation of China (grant number 21436008), the General Program of National Natural Science Foundation of China (grant number 51372162) and the Program for San Jin Scholars of Shanxi Province of China (2013).

Conflicts of Interest: The authors declare no conflict of interest.

References

1. Jost, H. Tribology—Origin and future. *Wear* **1990**, *136*, 1–17. [[CrossRef](#)]
2. Tomala, A.; Ripoll, M.R.; Gabler, C.; Remškar, M.; Kalin, M. Interactions between MoS₂ nanotubes and conventional additives in model oils. *Tribol. Int.* **2017**, *110*, 140–150. [[CrossRef](#)]
3. Yi, M.; Zhang, C. The synthesis of MoS₂ particles with different morphologies for tribological applications. *Tribol. Int.* **2017**, *116*, 285–294. [[CrossRef](#)]
4. Hu, E.Z.; Xu, Y.; Hu, K.H.; Hu, X.G. Tribological properties of 3 types of MoS₂ additives in different base greases. *Lubr. Sci.* **2017**, *29*, 1–15. [[CrossRef](#)]
5. Quan, X.; Zhang, S.; Hu, M.; Gao, X.; Jiang, D.; Sun, J. Tribological properties of WS₂/MoS₂-Ag composite films lubricated with ionic liquids under vacuum conditions. *Tribol. Int.* **2017**, *115*, 389–396. [[CrossRef](#)]
6. Aldana, P.U.; Vacher, B.; Mogne, T.L.; Belin, M.; Thiebaut, B.; Dassenoy, F. Action Mechanism of WS₂ Nanoparticles with ZDDP Additive in Boundary Lubrication Regime. *Tribol. Lett.* **2014**, *56*, 49–58. [[CrossRef](#)]
7. Zhou, L.H.; Wei, X.C.; Ma, Z.J.; Mei, B. Anti-friction performance of FeS nanoparticle synthesized by biological method. *Appl. Surf. Sci.* **2017**, *407*, 21–28. [[CrossRef](#)]
8. Zhang, Y.; Huang, B.; Li, P.; Wang, X.; Zhang, Y. Tribological performance of CuS-ZnO nanocomposite film: The effect of CuS doping. *Tribol. Int.* **2013**, *58*, 7–11. [[CrossRef](#)]
9. Liu, W.M.; Chen, S. An investigation of the tribological behaviour of surface-modified ZnS nanoparticles in liquid paraffin. *Wear* **2000**, *238*, 120–124. [[CrossRef](#)]
10. Chen, S.; Liu, W. Characterization and antiwear ability of non-coated ZnS nanoparticles and DDP-coated ZnS nanoparticles. *Mater. Res. Bull.* **2001**, *36*, 137–143. [[CrossRef](#)]
11. Min, Y.; Akbulut, M.; Prud'homme, R.K.; Golan, Y.; Israelachvili, J. Frictional properties of surfactant-coated rod-shaped nanoparticles in dry and humid dodecane. *J. Phys. Chem. B* **2008**, *112*, 14395–14401. [[CrossRef](#)] [[PubMed](#)]
12. Wang, L.B.; Gao, Y.P.; Li, Z.Y.; Zhou, A.G.; Li, P. Preparation and tribological properties of surface-modified ZnS nanoparticles. *Lubr. Sci.* **2015**, *27*, 241–250. [[CrossRef](#)]
13. Zhao, F.Y.; Li, G.T.; Zhang, G.; Wang, T.M.; Wang, Q.H. Hybrid effect of ZnS sub-micrometer particles and reinforcing fibers on tribological performance of polyimide under oil lubrication conditions. *Wear* **2017**, *380–381*, 86–95. [[CrossRef](#)]
14. Chang, L.; Zhang, Z.; Ye, L.; Friedrich, K. Tribological properties of high temperature resistant polymer composites with fine particles. *Tribol. Int.* **2007**, *40*, 1170–1178. [[CrossRef](#)]
15. Knör, N.; Gebhard, A.; Hauptert, F.; Schlarb, A.K. Polyetheretherketone (PEEK) nanocomposites for extreme mechanical and tribological loads. *Mech. Compos. Mater.* **2009**, *45*, 199–206. [[CrossRef](#)]
16. Yang, G.; Ma, H.; Wu, Z.; Zhang, P. Tribological behavior of ZnS-filled polyelectrolyte multilayers. *Wear* **2007**, *262*, 471–476. [[CrossRef](#)]
17. Guo, Y.B.; Wang, D.G.; Liu, S.H.; Zhang, S.W. Synthesis and tribological properties of CuS/ZnS nanoparticles doped polyelectrolyte multilayers. *Surf. Eng.* **2013**, *29*, 17–22. [[CrossRef](#)]
18. Kang, J.J.; Wang, C.B.; Wang, H.D.; Xu, B.S.; Liu, J.J.; Li, G.L. Research on tribological behaviors of composite Zn/ZnS coating under dry condition. *Int. Vac. Congr.* **2010**, *285*, 1940–1943. [[CrossRef](#)]
19. Ouyang, X.; Tsai, T.Y.; Chen, D.H.; Huang, Q.J.; Cheng, W.H.; Clearfield, A. Ab initio structure study from in-house powder diffraction of a novel ZnS(EN)_{0.5} structure with layered wurtzite ZnS fragment. *Chem. Commun.* **2003**, *7*, 886–887. [[CrossRef](#)]
20. Zhou, G.; Wang, X.; Yu, J. A low-temperature and mild solvothermal route to the synthesis of wurtzite-type ZnS with single-crystalline nanoplate-like morphology. *Cryst. Growth Des.* **2005**, *5*, 1761–1765. [[CrossRef](#)]
21. Chen, L.; Zhang, X.; Xu, H.; Dong, J. Tribological Investigation of Two Different Layered Zirconium Phosphates as Grease Additives under Reciprocating Sliding Test. *Tribol. Lett.* **2016**, *64*. [[CrossRef](#)]
22. Rudnick, L.R. *Lubricant Additives: Chemistry and Applications*; CRC Press: Boca Raton, FL, USA, 2009.
23. Zhao, H.; Huang, X.; Wang, J.; Li, Y.; Liao, R.; Wang, X.; Qiu, G. Comparison of bioleaching and dissolution process of p-type and n-type chalcopyrite. *Miner. Eng.* **2017**, *109*, 153–161. [[CrossRef](#)]
24. Wen, Z.; Xia, Y.; Liu, Z. Tribological Behavior and Mechanism of Overbased Complex Calcium Sulfonate Grease. *Acta Pet. Sin.* **2013**, *29*, 145–150.

25. Gong, K.; Wu, X.; Zhao, G.; Wang, X. Tribological properties of polymeric aryl phosphates grafted onto multi-walled carbon nanotubes as high-performances lubricant additive. *Tribol. Int.* **2017**, *116*, 172–179. [[CrossRef](#)]
26. Chen, X.J.; Xu, H.F.; Xu, N.S.; Zhao, F.H.; Lin, W.J.; Lin, G.; Fu, Y.L.; Huang, Z.L.; Wang, K.Z.; Wu, M.M. Wurtzite ZnS nanosaws produced by polar surfaces. *Chem. Phys. Lett.* **2004**, *385*, 8–11.
27. Chen, X.; Xu, H.; Xu, N.; Zhao, F.; Lin, W.; Lin, G.; Wu, M. Kinetically Controlled Synthesis of Wurtzite ZnS Nanorods through Mild Thermolysis of a Covalent Organic–Inorganic Network. *Inorg. Chem.* **2003**, *42*, 3100–3106. [[CrossRef](#)]



© 2019 by the authors. Licensee MDPI, Basel, Switzerland. This article is an open access article distributed under the terms and conditions of the Creative Commons Attribution (CC BY) license (<http://creativecommons.org/licenses/by/4.0/>).